

## Suppression and promotion of charge inversion in the presence of multivalent coions

Zhi-Yong Wang,<sup>1,2,\*</sup> Zengwei Ma,<sup>1</sup> and Yu-qiang Ma<sup>2,3</sup>

<sup>1</sup>*School of Optoelectronic Information, Chongqing University of Technology, Chongqing 400054, China*

<sup>2</sup>*National Laboratory of Solid State Microstructures, Nanjing University, Nanjing 210093, China*

<sup>3</sup>*Center for Soft Condensed Matter Physics and Interdisciplinary Research, Soochow University, Suzhou 215006, China*

(Received 24 September 2015; published 29 December 2015)

We report charge inversion using Monte Carlo calculations for a negatively charged surface in aqueous solutions involving coions of different charges and monovalent counterions. It is shown that a rise in the valence of coions at moderate concentrations can substantially promote charge inversion for the surface charge values of biological relevance, regardless of the representation of surface charges but dependent in a nontrivial way on polarization effects resulting from dielectric discontinuity. These obtained characteristics challenge the traditional belief that the coions are generally considered to suppress charge inversion and expose the important role of coions of higher valence in tailoring the effective interactions of biomolecules with the cell membrane.

DOI: [10.1103/PhysRevE.92.060303](https://doi.org/10.1103/PhysRevE.92.060303)

PACS number(s): 82.45.Gj, 68.08.De, 87.10.Rt, 82.70.-y

The electrostatics is rich and complex in soft matter and plays a significant role in phenomena such as charge inversion which occurs when a charged particle binds so many counterions that its effective charge reverses polarity [1]. It has been recognized that this anomalous effect underlies like-charge attraction, such as colloidal aggregation [2] and DNA condensation [3,4]. Despite long-standing efforts, the mechanisms behind charge inversion remain an issue of contention and our understanding of this topic is still far from being complete [5–19].

Most of our knowledge about charge inversion comes from the case where the counterions are multivalent, meaning that the charged particles can be more effectively overcompensated by multivalent counterions in solution due to electrostatic and excluded volume correlations as well as specific ion binding. Most recently, Faraudo and coauthors even established that monovalent ions with hydrophobic groups result in charge inversion of colloids [20]. In their subsequent publications [21,22], these authors further observed the hydrophobic effect is so strong that giant charge inversion occurs. By contrast, very few studies have been performed specifically to evaluate the role of coions in the structure of electric double layers [23–25] thanks to the conventional belief that multivalent coions adsorb onto the particle surfaces only weakly or not at all. To the best of our knowledge, no information is currently available on the contributions of multivalent coions to charge inversion besides an exception [26] where Patra considered a highly charged nanoparticle immersed in a mixture of mono- and divalent coions. Therefore, the aim of this Rapid Communication is to fill this gap and specifically to study how charge inversion is affected by the magnitude and representation of surface charges, salt concentration, as well as by polarization effects arising from dielectric discontinuity. To pursue this objective, we conduct a series of Monte Carlo simulations within the restricted primitive model of electrolytes.

Consider a substrate in the half space  $z < 0$  described by a permittivity  $\epsilon_< = 2$  for a dielectric representing the repulsive image charge contributions or by  $\epsilon_< = \infty$  for a conductor denoting the attractive image charge interactions. The surface

of this substrate at  $z = 0$  is assumed to be impenetrable and negatively charged, either having a homogeneous charge density  $\sigma_0$  or being decorated by a square array of hard spheres of radius  $2 \text{ \AA}$  whose centered monovalent point charges are placed on the surface with  $x$  and  $y$  coordinates in the corners of the array. The half space  $z > 0$  is the region of aqueous solution of a dielectric constant  $\epsilon_> = 80$ . The ideal case of  $\epsilon_< = \epsilon_> = 80$  corresponds to the situation of no image charges. Ions are considered as charged hard spheres of the radius of  $3.2 \text{ \AA}$  subject to moderate hydration based on the fact that ionic hydration numbers at interfaces are lower than those in the bulklike area [27], which interact with both electrostatic potential and contact repulsion. For more details, readers may refer to our earlier publication [28]. The Lekner method as modified for systems with slab geometry was applied to tackle the long-range Coulomb interactions [29]. All simulations with the overall electroneutrality condition were performed in the canonical ensemble at  $T = 298 \text{ K}$  employing the Metropolis scheme with periodic boundary conditions imposed in the  $x$  and  $y$  directions [30]. Also, system size effects were monitored and no detectable difference was observed.

To measure the screening of the surface's native charges by the ions, we calculate the cumulative charge density,  $\sigma_{\text{int}}(z) = \sigma_0 + \int_0^z dz' \sum_k Z_k e \rho_k(z')$ , where  $e$  is the elementary charge,  $Z_k$  is the valence of ionic species  $k$ , and  $\rho_k(z')$  is its local density at a distance  $z'$  from the surface. Since  $\sigma_0 < 0$  throughout, charge inversion appears when  $\sigma_{\text{int}}(z)$  changes the sign from negative to positive at some intermediate separations. Figure 1 presents  $\sigma_{\text{int}}(z)$  adjacent to a uniformly charged surface for two different charge values, in contact with a  $+1:-3$  type salt at varying concentrations in the absence and presence of the repulsive image charge contributions. For comparison, we also display the system of a  $+3:-1$  type electrolyte under the same conditions.

Let us begin by looking at the case of no image charges. What is more surprising from Fig. 1(a) is that at 240 mM, charge inversion in the system of multivalent coions becomes more robust than in the system of multivalent counterions, as indicated by a larger peak value and a more apparent oscillation in the dashed  $\sigma_{\text{int}}(z)$  curve in blue than the one in red. Moreover, the onset of charge inversion even resides closer to the surface in the system of multivalent coions. The

\*wzyong@cqut.edu.cn

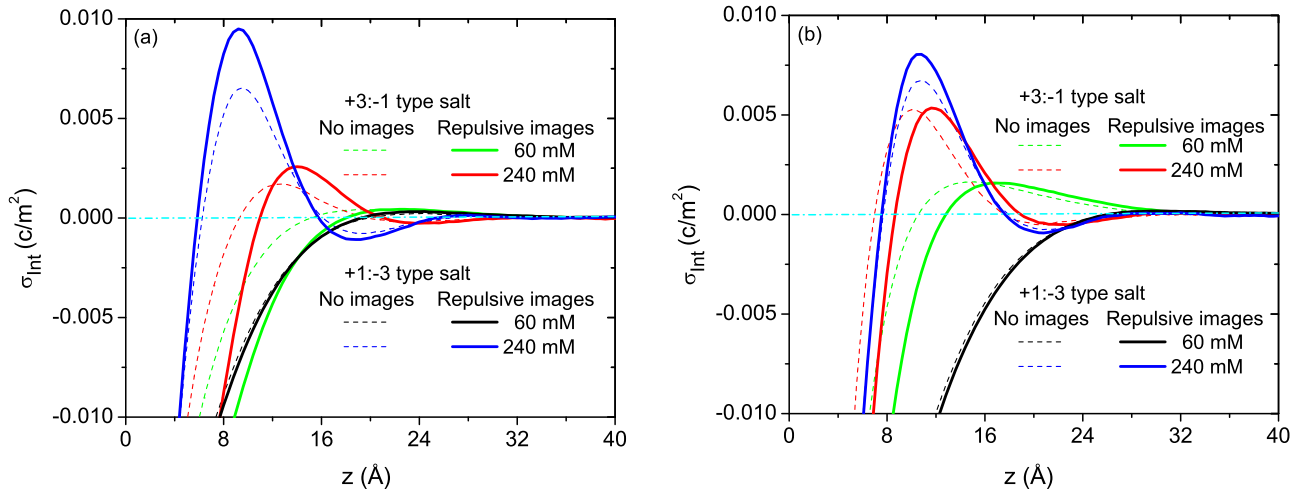


FIG. 1. (Color online) Averaged cumulative charge density next to a uniformly charged surface for (a)  $\sigma_0 = -0.02 \text{ C/m}^2$  and (b)  $\sigma_0 = -0.04 \text{ C/m}^2$  in contact with a +1:-3 type electrolyte at two different concentrations in the absence (dashed lines) and presence (solid lines) of repulsive images. Additional data are given for comparison by considering the frequently studied case where multivalent ions have the opposite charge as the substrate.

characteristics can be easily explained by the local density profiles of components in solution. As seen from Fig. 2(a), there is a more significant depletion of multivalent coions than monovalent coions in the immediate vicinity of the surface. In contrast, a more collapse occurs of monovalent counterions than multivalent counterions despite the fact that trivalent counterions are much more strongly attracted. It should be borne in mind that Fig. 2(a) displays normalized profiles. Although  $\rho_k/\rho_{k0}$  seems to be smaller for monovalent counterions in the surface region,  $\rho_k$  could be greater since the actual content of monovalent counterions is three times larger than that of trivalent counterions. This can be further shown by the observation that, in comparison to the +3:-1 type system, there is a much higher concentration of coions in the +1:-3 type system in a certain region of the double layer, which is due to the larger like-charges that are brought to the interface by an excess enrichment of monovalent counterions. In both systems, there exists a crossover on the density profiles of the counterions and the coions, being an important indicator

of charge inversion. The position of the crossover point where the coion density begins to exceed the counterion density supports a consistent picture of the onset of charge inversion.

Overall, Fig. 1(b) shows that the multivalent coion effect decreases at the slightly high surface charge density. At 60 mM, the dashed  $\sigma_{\text{int}}(z)$  curve in green passes through the electroneutral line, indicating the appearance of charge inversion in the system of multivalent counterions. As far as the system of multivalent coions is concerned, however, the black dashed  $\sigma_{\text{int}}(z)$  curve monotonically approaches zero, meaning that no charge inversion is observed. As salinity increases to 240 mM, the onset of charge inversion in the +3:-1 type system shifts towards the substrate and develops closer to the surface than in the +1:-3 type system, contrary to the foregoing analyses of  $\sigma_0 = -0.02 \text{ C/m}^2$ . These differences all reveal that multivalent counterions are significantly enhanced in the region very adjacent to the surface when the interfacial charge density becomes larger in magnitude.

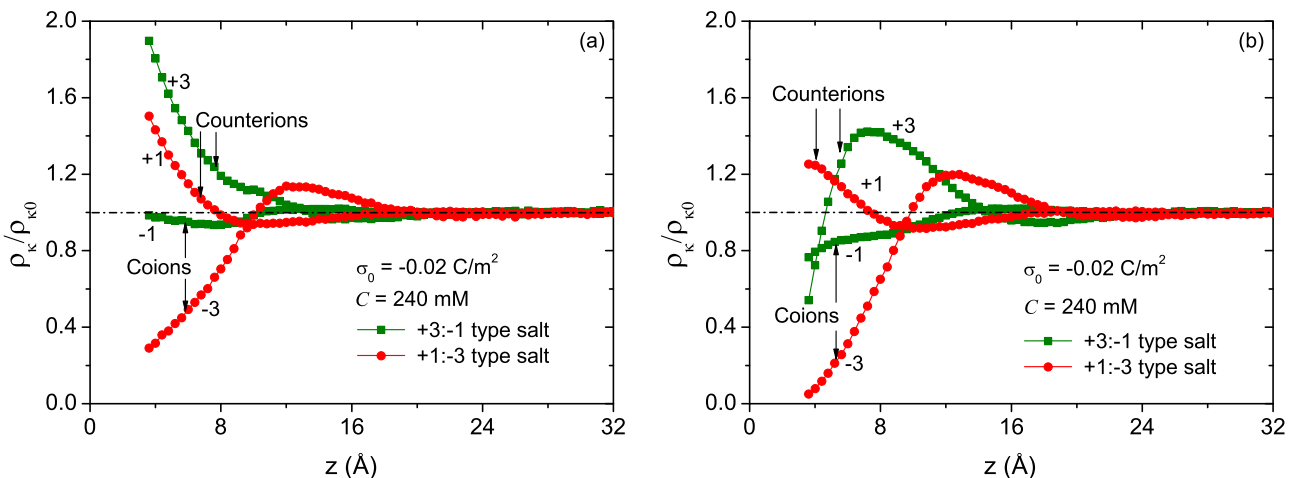


FIG. 2. (Color online) Averaged density profiles of components normalized to bulk values for various salts at  $C = 240 \text{ mM}$  and  $\sigma_0 = -0.02 \text{ C/m}^2$  in the absence (a) and presence (b) of repulsive images.

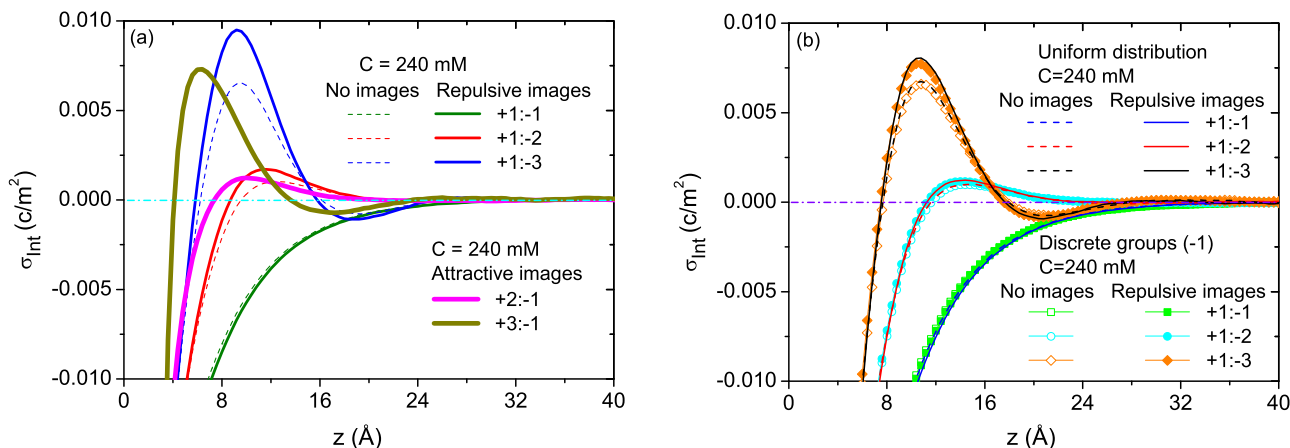


FIG. 3. (Color online) Averaged cumulative charge density for the coions of various valences at the same concentration of 240 mM without (dashed lines) and with (solid line) repulsive image charges in action. (a)  $\sigma_0 = -0.02 \text{ C/m}^2$  based on the assumption of the uniformly charged surface. For further stressing the promotion of charge inversion in the presence of multivalent coions, the case of attractive images is covered considering multivalent counterions. (b)  $\sigma_0 = -0.04 \text{ C/m}^2$  for various surface charge representations.

When polarization effects are present, Fig. 1 indicates that all the  $\sigma_{\text{int}}(z)$  curves in the case of multivalent counterions exhibit an obvious depletion effect due to the action of repulsive image charge forces. Interestingly, charge inversion in the presence of image charges instead becomes much stronger for  $\sigma_0 = -0.02 \text{ C/m}^2$  at 240 mM, as shown by a higher peak in the red solid  $\sigma_{\text{int}}(z)$  curve, than the case where polarization effects are absent. The variation in the local densities of the various ions in solution correlates well with the evolution of the cumulative charge density. We can clearly see that in Fig. 2(b), the  $\rho_k/\rho_{k0}$  curve in olive shows the expected depletion of multivalent counterions, but followed by the structure of a counterion-rich sublayer outside the depletion zone, which possesses a greater population of multivalent counterions than the ideal case of no image charges as already displayed in Fig. 2(a). This dense collapse may therefore lead to a more apparent charge inversion at some relative larger separations from the surface. Similar behavior was reported in our earlier publication for a surface of  $\sigma_0 = -0.04 \text{ C/m}^2$  immersed in a mixture of electrolytes of the +1:-1 and +3:-1 types, where the discrete interfacial groups are believed to play an important role [31]. However, it is noted from Fig. 1(b) that this anomalous effect vanishes when the charges are uniformly smeared out on the surface.

Most importantly, we discover from Fig. 1 that replacing the multivalent counterions by the multivalent coions yields a completely different scenario. At 60 mM, the  $\sigma_{\text{int}}(z)$  curves basically remain unchanged by the consideration of polarization effects, regardless of the magnitude of surface charge density. At 240 mM, apart from the finding that polarization effects exert a dramatic influence on the enhancement of charge inversion, we unexpectedly observe that the onset of charge inversion is located closer to the surface than the ideal case of no images, opposite to the trend observed in the system of the +3:-1 type electrolyte. However, the multivalent coion effects become less significant at the larger surface charge value because the double layer structure begins to be dominated through increasing electrostatic correlations.

Aiming to specifically elaborate the underlying physics at  $\sigma_0 = -0.02 \text{ C/m}^2$ , Fig. 2(b) depicts the density profile of

each component in red symbols along the  $z$  direction. As is clear, there is still a surface excess of monovalent counterions compared to the bulk despite image repulsions. On the other hand, the multivalent coions are strongly depleted from the close vicinity of the surface due to their higher valence so that almost no coions are found there. It is the enrichment of monovalent counterions in the interfacial region that induces the occurrence of excess multivalent coions in the next sublayer. This causes the coion concentration to locally exceed the counterion concentration at some intermediate separations. Moreover, the degree that the amount of multivalent coions is greater than that of monovalent counterions is more appreciable when compared to the ideal case without image charges, as already revealed in Fig. 2(a) still in red symbols, implying a stronger charge inversion when repulsive image charges are present.

To demonstrate the coion's predominant role in promoting charge inversion, Fig. 3 focuses on the response of  $\sigma_{\text{int}}(z)$  to the valence of coions with reference to the same surface charge magnitudes above. Overall, charge inversion is gradually promoted with an increase in the charge of coions, and polarization effects become more favorable in a similar manner as well despite a reduction in the intensity with increasing surface charge density. It should be pointed out that the spectra in Fig. 3(b) unveil that the discretization of surface charges has a negligible influence on charge inversion. The same regularity is also observed for  $\sigma_0 = -0.02 \text{ C/m}^2$  (data not shown). It is of particular interest to note from Fig. 3(a) that in the system of trivalent coions, the  $\sigma_{\text{int}}(z)$  curve anomalously shows a higher peak in the presence of the repulsive image charge contributions than the system where the counterions are trivalent with attractive images in action, implying a stronger charge inversion in the former case although the onset of charge inversion approaches the surface closer in the latter due to favorable image attractions. The same trend continues further in the system of divalent coions but the strength becomes less conspicuous. Below, we only take the case of trivalent coions as an example to illustrate the counterintuitive behavior from the averaged number densities of the various ionic species.

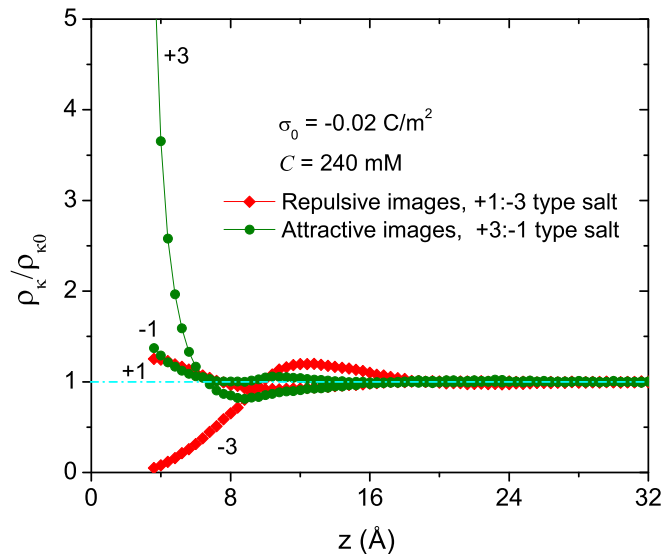


FIG. 4. (Color online) A comparison of the normalized density profiles of various species close to a surface of  $\sigma_0 = -0.02$  C/m<sup>2</sup> at  $C = 240$  mM for different types of salts and images.

According to Fig. 4, there is a sharp peak of trivalent counterion at its contact plane in the case of the +3:−1 type electrolyte under the action of attractive image forces, and the monovalent coions are substantially enriched as well at the surface immediate region. Taken together, the total amount of accumulated charges is, however, less than that in the case of the +1:−3 type salt with repulsive image charges in action, where the trivalent coions are almost completely excluded from the inmost interfacial region but the monovalent counterions still concentrate there. Note that whichever the case, the content of monovalent ions is three times that of trivalent ions. Furthermore, we observe that the location of the initial crossover point on the density profiles of the counterions and the coions in the case of trivalent counterions situates closer to the surface when compared to the case of trivalent coions, showing a remarkable degree of consistency in predicting the onset of charge inversion in terms of the  $\sigma_{\text{int}}(z)$  curves.

Figure 5 records the cumulative charge density under the same conditions as Fig. 1 but for a highly charged surface of  $\sigma_0 = -0.16$  C/m<sup>2</sup>. Still, charge inversion is enhanced with the increase of salt amount, irrespective of the salt type. In this regard, our finding in the case of multivalent coions agrees with what was observed for the structure of colloidal solution at varying concentration ratio of mono- and divalent coions of mixed electrolytes [26]. No matter how many salts are present in solution, charge inversion becomes more pronounced when the counterions are multivalent due to the strong electrostatic coupling between surface charges and multivalent counterions, and the onset of charge inversion shifts closer to the surface in comparison to the case where the coions are multivalent. Moreover, the  $\sigma_{\text{int}}(z)$  curve in the +3:−1 type system at 60 mM exhibits a higher peak than the one in the +1:−3 type system at 240 mM. These observations unequivocally reveal that charge inversion is largely suppressed in the presence of multivalent coions at the larger value of surface charge density, returning to the traditional belief. Another feature of Fig. 5 is

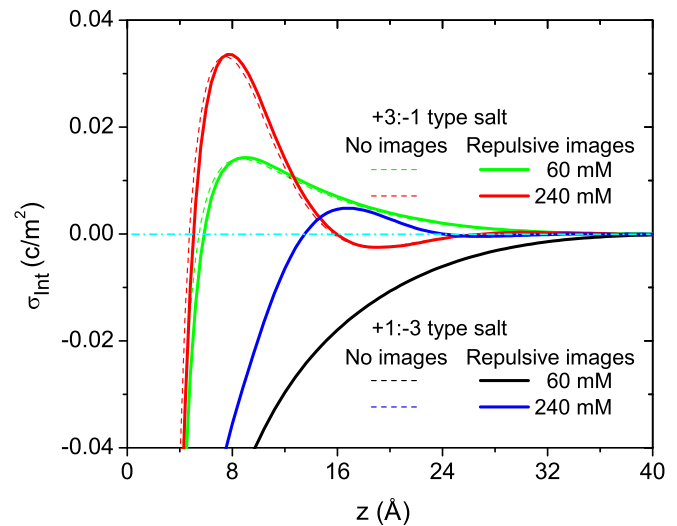


FIG. 5. (Color online) As for Fig. 1 but with  $\sigma_0 = -0.16$  C/m<sup>2</sup>.

that all  $\sigma_{\text{int}}(z)$  curves become less sensitive to polarization effects, independent of the type of electrolyte. This is mainly a consequence of the repulsive image charge contributions being thoroughly restrained by the cooperative interplay between the steric repulsion of ions and the strong correlation effects.

In conclusion, we have elaborated at a fundamental level the missing understanding on the key role of multivalent coions in ion accumulation near interfaces. When the surface to be investigated is weakly charged, our findings show unambiguous evidence of the importance of the coion's valence in promoting charge inversion at moderate salinity, which can be further boosted by the action of polarization effects, refuting the conventional claim that both the coions and the repulsive image charge forces are generally considered to depress charge inversion. In contrast to the frequently studied situation of multivalent counterions, on the other hand, charge inversion in the presence of multivalent coions is damped rapidly with increasing magnitude of the surface charges. Since the overall charge density on a typical biological membrane ranges from  $-0.01$  to  $-0.05$  C/m<sup>2</sup> [32,33], this work therefore holds great relevance in biological systems where small proteins can play the role of multivalent coions and, in order to grasp physicochemical processes occurring at the membrane surface, it is necessary to consider dielectric discontinuity between the aqueous environment ( $\epsilon_s \approx 80$ ) and the hydrocarbon interior ( $\epsilon_c \approx 2$ ). In parallel, our study of the basic physics of multivalent coion-promoted charge inversion might provide interesting insight into possible mechanisms for tailoring colloidal interactions in solutions via salt effects [34,35] and help to give rise to more applied problems of technological relevance [12].

Z.-Y. thanks Dr. Chun-lai Ren for valuable discussions. This research is funded by the National Natural Science Foundation of China (Grants No. 11104364 and No. 21304110), by Chongqing Research Program of Basic Research and Frontier Technology (Grant No. cstc2015jcyjBX0056) and partially by the Scientific and Technological Research Program of Chongqing Municipal Education Commission (Grant No. KJ1400921).

- [1] U. P. Strauss, N. L. Gershfeld, and H. Spiera, *J. Am. Chem. Soc.* **76**, 5909 (1954).
- [2] R. Messina, C. Holm, and K. Kremer, *Phys. Rev. Lett.* **85**, 872 (2000).
- [3] K. Besteman, K. Van Eijk, and S. G. Lemay, *Nat. Phys.* **3**, 641 (2007).
- [4] G. C. L. Wong and L. Pollack, *Annu. Rev. Phys. Chem.* **61**, 171 (2010).
- [5] H. Boroudjerdi, Y.-W. Kim, A. Naji, R. R. Netz, X. Schlagberger, and A. Serr, *Phys. Rep.* **416**, 129 (2005).
- [6] Y. Levin, *Rep. Prog. Phys.* **65**, 1577 (2002).
- [7] R. Messina, *J. Phys.: Condens. Matter* **21**, 113102 (2009).
- [8] A. Y. Grosberg, T. T. Nguyen, and B. I. Shklovskii, *Rev. Mod. Phys.* **74**, 329 (2002).
- [9] E. Wernersson, R. Kjellander, and J. Lyklema, *J. Phys. Chem. C* **114**, 1849 (2010).
- [10] R. Qiao and N. R. Aluru, *Phys. Rev. Lett.* **92**, 198301 (2004).
- [11] D. F. Parsons and B. W. Ninham, *Langmuir* **26**, 6430 (2010).
- [12] S. X. Li, W. Guan, B. Weiner, and M. A. Reed, *Nano Lett.* **15**, 5046 (2015).
- [13] W. Wang, R. Y. Park, A. Travesset, and D. Vaknin, *Phys. Rev. Lett.* **106**, 056102 (2011).
- [14] J. Faraudo and A. Travesset, *J. Phys. Chem. C* **111**, 987 (2007).
- [15] A. Martín-Molina, C. Rodríguez-Beas, and J. Faraudo, *Phys. Rev. Lett.* **104**, 168103 (2010).
- [16] C. Calero and J. Faraudo, *Phys. Rev. E* **80**, 042601 (2009).
- [17] M. Deserno, F. Jiménez-Ángeles, C. Holm, and M. Lozada-Cassou, *J. Phys. Chem. B* **105**, 10983 (2001).
- [18] K. Besteman, M. A. G. Zevenbergen, and S. G. Lemay, *Phys. Rev. E* **72**, 061501 (2005).
- [19] S. Buyukdagli, R. Blossey, and T. Ala-Nissila, *Phys. Rev. Lett.* **114**, 088303 (2015).
- [20] A. Martín-Molina, C. Calero, J. Faraudo, M. Quesada-Pérez, A. Travesset, and R. Hidalgo-Álvarez, *Soft Matter* **5**, 1350 (2009).
- [21] C. Calero and J. Faraudo, *J. Am. Chem. Soc.* **133**, 15025 (2011).
- [22] L. Pérez-Fuentes, C. Drummond, J. Faraudo, and D. Bastos-González, *Soft Matter* **11**, 5077 (2015).
- [23] Z.-Y. Wang, Y.-P. Xie, Q. Liang, Z. Ma, and J. Wei, *J. Chem. Phys.* **137**, 174707 (2012).
- [24] B. Jamnik and V. Valchy, *J. Am. Chem. Soc.* **115**, 660 (1993).
- [25] E. R. A. Lima, M. Boström, D. Horinek, E. C. Biscaia, W. Kunz, and F. W. Tavares, *Langmuir* **24**, 3944 (2008).
- [26] C. N. Patra, *J. Phys. Chem. B* **114**, 10550 (2010).
- [27] M. Y. Kiriukhin and K. D. Collins, *Biophys. Chem.* **99**, 155 (2002).
- [28] Z.-Y. Wang and Y.-Q. Ma, *J. Chem. Phys.* **131**, 244715 (2009).
- [29] A. Grzybowski and A. Bródka, *Mol. Phys.* **100**, 1017 (2002).
- [30] M. P. Allen and D. J. Tildesley, *Computer Simulation of Liquids* (Oxford University Press, Oxford, 1987).
- [31] Z.-Y. Wang and Y.-Q. Ma, *J. Phys. Chem. B* **114**, 13386 (2010).
- [32] G. Ceve, *Biochim. Biophys. Acta* **1031**, 311 (1990).
- [33] W. F. Heinz and J. H. Hoh, *Biophys. J.* **76**, 528 (1999).
- [34] J.-P. Hansen and H. Löwen, *Annu. Rev. Phys. Chem.* **51**, 209 (2000).
- [35] T. Cao, I. Szilagy, T. Oncsik, M. Borkovec, and G. Trefalt, *Langmuir* **31**, 6610 (2015).